Kidney International, Vol. 68 (2005), pp. 938–947

GENETIC DISORDERS – DEVELOPMENT

Aprt/*Opn* double knockout mice: Osteopontin is a modifier of kidney stone disease severity

Hilary J. Vernon, Christine Osborne, Eleni G. Tzortzaki, Min Yang, Jianmen Chen, Susan R. Rittling, David T. Denhardt, Steven Buyske, Sharon B. Bledsoe, Andrew P. Evan, Lynette Fairbanks, H. Anne Simmonds, Jay A. Tischfield, and Amrik Sahota

Department of Genetics, Rutgers University, Piscataway, New Jersey; Department of Cell Biology and Neuroscience, Rutgers University, Piscataway, New Jersey; Department of Statistics, Rutgers University, Piscataway, New Jersey; Faculty of Medicine, University of Crete, Crete, Greece; Department of Anatomy and Cell Biology, Indiana University School of Medicine, Indianapolis, Indiana; and Purine Research Laboratory, Guy's Hospital, London, United Kingdom

***Aprt*/*Opn* double knockout mice: Osteopontin is a modifier of kidney stone disease severity.**

Background. Osteopontin (OPN) is reported to have two distinct functions in kidney disease: Promotion of inflammation at sites of tissue injury, and inhibition of calcium oxalate monohydrate stone formation. However, many of the studies supporting these functions were carried out in animal models of acute renal injury or in cultured cells; thus, the role of OPN in chronic renal disease is not well defined. We examined the role of OPN in adenine phosphoribosyltransferase (*Aprt*) knockout mice, in which inflammation and formation of 2,8-dihydroxyadenine (DHA) kidney stones are prominent features, by generating *Aprt*/*Opn* double knockout mice.

Methods. We characterized the phenotypes of six- and 12-week-old *Aprt*−/− *Opn*−/−, *Aprt*−/− *Opn*+/+, *Aprt*+/+ *Opn*−/−, and *Aprt*+/+ *Opn*+/+ male and female mice using biochemical, histologic, immunohistochemical, and in situ hybridization techniques.

Results. At 6 weeks of age, there was no difference in phenotype between double knockout and *Aprt* knockout mice. At 12 weeks, there was increased adenine and DHA excretion, renal crystal deposition, and inflammation in double knockout versus *Aprt* knockout male mice. Double knockout and *Aprt* knockout female mice at 12 weeks had less pathology than their male counterparts, but kidneys from double knockout females showed more inflammation compared with *Aprt* knockout females; both genotypes had similar levels of DHA crystal deposition.

Conclusion. We conclude that (*1*) OPN is a major inhibitor of DHA crystal deposition and inflammation in male mice; and (*2*) OPN is a major modifier of the inflammatory response but not of crystal deposition in female mice. Thus, separate mechanisms appear responsible for the tissue changes seen in DKO males versus females.

Key words: adenine phosphoribosyltransferase, 2,8-dihydroxyadenine, inflammation, kidney stone disease, osteopontin, xanthine dehydrogenase.

Received for publication September 19, 2004
and in revised form December 27, 2004, and March 7, 2005
Accepted for publication March 30, 2005

Many natural inhibitors of kidney stone formation have been identified in urine, but inhibitors affecting calcium oxalate monohydrate stone formation have been the most widely studied [1]. Urinary proteins with inhibitory activity include bikunin, osteopontin (OPN), prothrombin fragments, and Tamm-Horsfall protein [2–8]. Most of these proteins are anionic, with many acidic amino acid residues, and they frequently contain post-translational modifications such as phosphorylation or glycosylation. The inhibitors appear to bind to calcium oxalate surfaces [9], but the structural features that favor crystal binding and subsequent inhibition of stone formation are not fully understood. The inhibitory effects of OPN on stone formation are likely to be dependent on the phosphorylation state of OPN, with higher levels causing more inhibition of crystal nucleation and aggregation [10]. In normal mouse kidney, OPN expression was observed primarily in the thick ascending limbs of the loop of Henle and in distal convoluted tubules [11]. In human kidney, OPN expression has been observed in the descending loop of Henle, collecting ducts, and the renal papilla [12], sites that are considered to be associated with the onset of stone formation. An increase in OPN expression has been demonstrated in proximal tubular epithelium in humans following cyclosporine toxicity and in rodent models of renal injury [13], including kidneys from calcium oxalate monohydrate stone forming rats [14, 15]. OPN also is reported to be a promoter of tissue inflammation [13, 16–21]. OPN likely promotes inflammation via interaction with the CD44 receptor on macrophages and induction of chemotaxis, and via attachment to the β_3 integrin receptors and induction of cell spreading and activation [16, 21, 22].

Two knockout mouse models for OPN have been developed, including the one at our institution [23, 24]. *Opn* knockout mice appear anatomically normal, are fertile, show no size differences from their wild-type littermates,

and have histologically normal kidneys [13, 25]. However, they do show some phenotypic differences from wild-type mice, including resistance to ovariectomy-induced bone resorption [26] and parathyroid hormone (PTH)-induced enhancement of cortical bone formation [27]. Several models of acute renal injury, including ischemia [28], ureteral ligation [29], and cyclosporine toxicity [30], have been created in these mice. These models all demonstrated more macrophage infiltration in wild-type mice compared with *Opn* knockout mice, suggesting that OPN is a promoter of inflammation in the kidney. OPN also has renoprotective effects, as demonstrated by significantly more blood urea nitrogen (BUN) and creatinine retention and increased structural renal damage following ischemia in *Opn* knockout mice compared with wild-type mice [25]. Following ethylene glycol–induced hyperoxaluria, there was significant intratubular deposition of calcium oxalate monohydrate crystals in *Opn* knockout mice, whereas wild-type mice were unaffected, further supporting a renoprotective role for OPN [31]. In a mouse model of mycobacterial infection, *Opn* knockout mice had more severe infections and greater granuloma burden, suggesting that the protective effects of OPN are not limited to the kidney [32].

Many of the studies supporting the proinflammatory and the stone-inhibiting properties of OPN have been carried out in animal models of acute renal injury or in cultured cells. These models are not appropriate for chronic kidney diseases, such as hereditary stone disease, where the disease process may have been active since birth. Over 30 hereditary stone diseases have been recognized [33], including kidney stones associated with hypercalciuria, hypophosphatemia, hyperoxaluria, cystinuria, hyperuricosuria, and xanthinuria [34]. Our laboratory has been investigating another genetic disorder—adenine phosphoribosyltransferase (APRT) deficiency—in which kidney stone disease is a major phenotype [35]. APRT catalyzes the synthesis of adenosine monophosphate (AMP) from adenine, but in APRT deficiency adenine is oxidized by xanthine dehydrogenase (XDH)—via the intermediate 8-hydroxyadeine (HA)—to 2,8-dihydroxyadenine (DHA). DHA is highly insoluble at normal urine pH and this can lead to crystal aggregation and stone formation in many APRT-deficient patients [36]. We previously generated *Aprt* knockout mice [37, 38], and we have used these mice to identify some of the early cellular and molecular events involved in kidney stone formation [39–42]. These mice show DHA crystals in the collecting ducts as early as 2 days of age, and older mice have crystal deposition throughout the renal system as well as high levels of inflammation and tissue fibrosis [43]. We also observed increased OPN mRNA expression in kidney sections from these mice [Tzortzaki et al, unpublished data], suggesting that OPN may be one of the initial protective responses of the kidney to the presence of crystals.

In this study, we examined the role of OPN in DHA kidney stone formation by creating *Aprt*/*Opn* double knockout mice. We hypothesized that if one of the major roles of OPN is the inhibition of crystal aggregation and stone formation in the urinary tract, then the onset of stone disease would be earlier or the phenotype more severe in double knockout mice compared with *Aprt*−/− mice. The increased crystal burden in the double knockout mice would also be expected to lead to increased inflammation in these mice. We studied both male and female mice, given the gender differences in the prevalence of kidney stones [44–46]. Mice of all four genotypes (*Aprt*−/− *Opn*−/−, *Aprt*−/− *Opn*+/+, *Aprt*+/+ *Opn*−/−, and *Aprt*+/+ *Opn*+/+) were examined at 6 and 12 weeks of age using biochemical, histologic, immunohistochemical, and in situ hybridization techniques. These age groups were selected because at 6 weeks inflammation is first seen to develop in Aprt-deficient male mice, and at 12 weeks inflammation and fibrosis are severe in male mice and also evident in female mice [37, 43].

METHODS

Mouse breeding, DNA extraction, and genotyping

Animal studies were approved by the Rutgers University Institutional Animal Care and Use Committee. Strain 129 mice of genotypes *Aprt*−/− *Opn*+/+ [37] and *Aprt*+/+ *Opn*−/− [24] were mated to generate *Aprt*+/− *Opn*+/− mice, which were then interbred to create *Aprt*−/− *Opn*−/− mice. DNA was extracted from mice tails at weaning and the genotypes at the *Aprt* and *Opn* loci determined using allele-specific polymerase chain reaction (PCR) [24, 47]. To examine the effects of *Opn* background on mouse survival, pups born to *Aprt* heterozygous parents that were homozygous +/+ or −/− for *Opn* were genotyped, and the observed and expected genotype frequencies compared using chi square.

Weight and growth analysis

Male and female mice of all four genotypes were weighed on a weekly basis from weaning to 12 weeks of age. Each genotype included at least six mice of each gender. Data were analyzed for rate of weight change, range of change (maximum minus minimum weight), and maximum achieved weight using growth curves fitted to Gompert's growth formula:

$$\text{Weight} = \text{Asymptote}^{-b_2 b_3 \wedge \text{age}}$$

where b_2 and b_3 are the rate and range of weight change, respectively, and the asymptote is the maximum weight.

Urine collection and analysis

Urine samples were collected in individual metabolic cages (Braintree Scientific, Braintree, MA, USA); mice

had free access to water and food during the collection process. Approximately 400 μL urine was collected from each mouse over a 4- to 16-hour period. Urine was stored at −20°C until shipped overnight on dry ice to Guy's Hospital, London, for analysis by reverse-phase high-performance liquid chromatography (HPLC) [48]. The analytes quantified included creatinine, uric acid (UA), hypoxanthine (H), xanthine (X), adenine (A), HA, and DHA. The data were expressed as total adenines (A, HA, and DHA) as a fraction of total purines (UA, H, X, A, HA, DHA) and DHA as a fraction of total adenines, and all values were normalized to creatinine. Data for the *Aprt* and *Aprt*/*Opn* knockout mice were compared using the unpaired *t test*.

Tissue harvesting, crystal quantification, and histologic evaluation

Mice were anesthetized, the left kidney removed and frozen for crystal quantification, and the right kidney perfused and embedded in paraffin for histologic studies, as previously described [43]. Briefly, crystal quantification was carried out by examining kidney sections under polarized light with a Leica DMA microscope (Leica Microsystems, Bannockburn, IL, USA) and scanning with a Polaroid DMA digital camera (Polaroid Corp., Waltham, MA, USA). The birefringent DHA crystals were identified, and the total particle area calculated. The average crystal area was determined from six sections from each mouse. Renal pathology was graded on a scale of 0 to 5 for each of ten pathologic parameters, with 0 denoting not affected and 5 as severely affected, as reported elsewhere by our group [43]. The parameters included tubular atrophy, tubular dilation, tubular debris, tubular necrosis, tubular hyperplasia, micropolyps, interstitial nephritis, macrophage infiltration, glomerular sclerosis, and vascular sclerosis. Scores were recorded by two investigators blinded to the identity of the mice, and the scores were then averaged.

Immunohistochemistry and macrophage quantification

Immunohistochemistry was performed with rat antimouse antibody to the macrophage epitope F4/80 (Caltag Laboratories, Burlingame, CA, USA) using reagents from Vector Laboratories (Burlingame, CA, USA). Slides were dewaxed, rehydrated, and endogenous peroxidases blocked with 0.3% hydrogen peroxide. Tissue sections were blocked in 1:20 dilution of rabbit serum, and 70 μL of F4/80 antibody at a dilution of 1:250 was then applied to each section overnight at 4°C. Sections with no primary antibody were used as negative controls. Secondary biotinylated rabbit antirat antibody at a concentration of 5 μg/mL was applied for 1 hour, followed by freshly prepared ABC reagent for 1 hour. 3,3′-diaminobenzidine (DAB) reagent (Sigma Fast 3,3′-Diaminobenzidine Tablet Set) (Sigma Chemical Co., St. Louis, MO, USA) was then applied for 2 minutes to each section, and, after a water wash, the sections were stained with hematoxylin, Gills formulation #2 (Fisher Scientific, Fair Lawn, NJ, USA). Slides were dehydrated, cleared in xylene, mounted with Cytoseal (Stephens Scientific, Kalamazoo, MI, USA) and covered with FisherFinest glass coverslips (Fisher Scientific).

Slides were examined using a Nikon Eclipse E800 microscope (Nikon, Melville, NY, USA), and each section was given a score on a scale of 0 to 3. Scores were based on the following criteria: 0, no macrophages seen; 1, small single patch of macrophages occupying less than 10% of the section; 2, >10% but <30% of the section showing macrophage infiltration; and 3, more than 30% macrophage infiltration. Two investigators who were blinded to the origin of the sections did the scoring independently, and the scores were averaged.

Picrosirius red staining and collagen quantification

Slides were dewaxed and rehydrated, stained for 1 hour in Direct Red 80 (0.05 g in 50 mL of saturated picric acid (Aldrich Chemical Co., Milwaukee, WI, USA), and then rinsed twice in 0.5% acetic acid. Slides were then dehydrated, cleared in xylene, and mounted. Slides were examined as above and five to eight images per section captured (at 10× magnification) using MagnaFire software (Optronics, Goleta, CA, USA) [39, 40]. This number of images was sufficient to capture the entire cortical region of each section. Area was measured using the Scion Image for Windows software (Scion, Fredrick, MD, USA), available free at *http://www.scioncorp.com* and at *http://rsb.info.nih.gov/nih-image/*. Collagen staining was quantified as a percentage of the entire kidney section.

XDH mRNA in situ hybridization

The sequences of the antisense and sense (used as a negative control) XDH oligonucleotide probes were CT GCATCCTGTCCAGGAGAGAATTGCCAAA, and TTTGGCAATTCTCTCCTGGACAGGATGCAG, respectively. The probes were labeled with fluorescein isothiocyanate (FITC) using a 5′ end labeling kit as described (Vector Laboratories). Slides were dewaxed, rehydrated, and washed in diethyl pyrocarbonate (DEPC)-treated phosphate-buffered saline (PBS) containing 100 mmol/L glycine. They were then placed in DEPC-treated PBS containing 0.3% Triton X-100, and each section treated with 50 μL of 5 μg/mL proteinase K for 15 minutes at 37°C. Slides were then incubated for 2 hours in 50 μL of prehybridization solution per section, followed by 15 ng/μL of sense or antisense probe overnight at 37°C. Slides were washed sequentially in 2×, 1×, and 0.25× standard sodium citrate (SSC) at 37°C, followed by incubation for 10 minutes with rabbit serum diluted 1:5 in Tris-buffered saline (TBS), 3% bovine serum albumin (BSA), and 0.1% Triton X-100.

Table 1. Expected and observed genotype ratios for female and male pups

		Opn+/+ background $N = 74$		*Opn*−/− background $N = 132$	
Aprt genotype	Expected	Females	Males	Females	Males
Aprt−/−	1	2	1	1	1
Aprt+/−	2	2.9	2.6	4.4	2.84
Aprt+/+	1	1	1.7	1.9	1.4
Chi square		2.9	1.29	28.6[a]	1.35

[a]Statistically significant. Chi-square for 2 degrees of freedom for a *P* value of 0.05 is 5.99.

Slides were then incubated with rabbit F(ab′) anti-FITC conjugated to alkaline phosphatase (NovoCastra Laboratories, Newcastle, UK) diluted 1:200 in TBS, 3% BSA, and 0.1% Triton X-100. After washing with TBS, slides were placed in alkaline phosphatase buffer for 5 minutes, and then incubated overnight in the dark at room temperature in this buffer containing 1% levamisole, 8% 5-bromo-5-chloro 3-indolyl phosphate, and 8% nitro blue tetrazolium. Slides were counterstained with eosin Y for 15 seconds, and immediately placed in 50% ethanol for 2 minutes. Slides were then dehydrated, cleared, mounted, and coverslipped as above.

RESULTS

Mouse survival

Mouse gender and genotypes were determined at 4 to 6 weeks of age. Any mice that died before this age were not included in the mouse survival survey; however, dead pups that we were able to genotype did not belong to any specific genotype group (unpublished observations). All pups were born to *Aprt*+/− parents either on an *Opn*+/+ or *Opn*−/− background (Table 1). The only group that differed significantly from Mendelian inheritance was female offspring born on an *Opn*−/− background (chi square 28.6, $P < 0.001$), suggesting that *Aprt*−/− *Opn*−/− female mice have lower survival than their *Aprt*−/− *Opn*+/+ counterparts.

Weight and growth

In male mice, the asymptote differed significantly for the *Aprt*−/− *Opn*+/+ and wild-type mice and for the *Aprt*−/− *Opn*−/− and wild-type mice, with wild-type mice having greater maximum weight in each case (*P* values 0.05 and <0.001, respectively). The asymptote also differed significantly for *Aprt*−/− *Opn*−/− and *Aprt*−/− *Opn*+/+ mice, with the latter having a greater maximum weight (*P* value 0.045). Females showed a different pattern of weight change compared with males: there was no difference for females in the maximum weight achieved among any of the genotypes, but parameters b_2 and b_3 varied among genotypes. Comparing the *Aprt*−/− *Opn*−/− and *Aprt*−/− *Opn*+/+ genotypes, for example, the former group had a smaller b_2 (*P* value 0.001) and a larger b_3 (*P* value <0.001), indicating that this group had a smaller range of weight gain. Since the asymptotes were not different, this suggested that at a young age the *Aprt*−/− *Opn*+/+ female mice were smaller, but gained weight faster and reached the same maximum weight as the *Aprt*−/− *Opn*−/− female mice.

Urine analysis

Males tended to produce more urine than females, and the urine output decreased in the order *Aprt*−/− *Opn*−/− > *Aprt*−/− *Opn*+/+ > *Aprt*+/+ *Opn*+/+, and *Aprt*+/+ *Opn*−/−. The ratio of total adenines/total purines and DHA/total adenines is a reflection of DHA formation and stone disease severity in the knockout mice, with higher ratios indicating more severe disease. We found no significant difference in these ratios between gender-matched groups of *Aprt*−/− *Opn*−/− and *Aprt*−/− *Opn* +/+ mice at 6 weeks of age. There was a statistically significant difference in purine excretion between males of genotypes *Aprt*−/− *Opn*−/− and *Aprt*−/− *Opn*+/+ at 12 weeks, with a *P* value of 0.039 for adenines/total purines and a *P* value of <0.001 for DHA/total adenines (Table 2). However, there was no significant difference in these ratios between female mice of genotypes *Aprt*−/− *Opn*−/− and *Aprt*−/− *Opn* +/+ at 12 weeks, although both sets of female animals excreted adenine and DHA at levels that were comparable to those in male mice of the same genotypes (Table 2). Mice of genotypes *Aprt*+/+ *Opn*+/+ and *Aprt*+/+ *Opn*−/− excreted trace amounts of adenine but no detectable amounts of DHA.

Pathology scores

Four to six mice of each gender, age, and genotype were examined for renal pathologic changes (Table 3). We found no significant difference in pathology scores between gender-matched male or female mice at age 6 weeks for genotypes *Aprt*−/− *Opn*−/− and *Aprt*−/− *Opn*+/+. The scores for 12-week-old male mice of genotypes *Aprt*−/− *Opn*−/− were higher (2.0 ± 0.79) compared with *Aprt*−/− *Opn*+/+ mice (0.9 ± 1.0), but the difference did not reach statistical significance in the small number of mice tested. There was a statistically significant difference in scores between 12-week-old females for genotypes *Aprt*−/− *Opn*−/− and *Aprt*−/− *Opn* +/+ (1.72 ± 1.20 versus 0.13 ± 0.25, *P* value 0.033). The *Aprt*+/+ *Opn*+/+ and *Aprt*+/+ *Opn*−/− mice showed no renal pathologic changes. We also noted that, in general, *Aprt*−/− females had lower pathology scores than males in matched genotype groups, regardless of *Opn* genotype, but the data were not statistically significant.

Table 2. Urinary purine content in mice by age, gender, and genotype

Genotype	Number	Gender	Age *weeks*	Adenines/purines	DHA/adenines
Aprt+/+ *Opn*+/+	3	Male	6	0.011 ± 0.010	–
Aprt+/+ *Opn*−/−	4	Male	6	0.009 ± 0.004	–
Aprt−/− *Opn*+/+	5	Male	6	0.67 ± 0.12	0.67 ± 0.11
Aprt−/− *Opn*−/−	6	Male	6	0.61 ± 0.16	0.66 ± 0.10
Aprt+/+ *Opn*+/+	5	Female	6	0.019 ± 0.012	–
Aprt+/+ *Opn*−/−	6	Female	6	0.018 ± 0.003	–
Aprt−/− *Opn*+/+	7	Female	6	0.43 ± 0.13	0.66 ± 0.09
Aprt−/− *Opn*−/−	6	Female	6	0.44 ± 0.08	0.65 ± 0.12
[a]*Aprt*+/+ *Opn*+/+	1	Male	12	–	–
Aprt+/+ *Opn*−/−	4	Male	12	0.029 ± 0.008	–
[b]*Aprt*−/− *Opn*+/+	6	Male	12	0.42 ± 0.22	0.54 ± 0.09
[b]*Aprt*−/− *Opn*−/−	6	Male	12	0.69 ± 0.16	0.77 ± 0.06
Aprt+/+ *Opn*+/+	3	Female	12	0.047 ± 0.008	–
Aprt+/+ *Opn*−/−	5	Female	12	0.050 ± 0.005	–
[c]*Aprt*−/− *Opn*+/+	6	Female	12	0.64 ± 0.18	0.83 ± 0.06
[c]*Aprt*−/− *Opn*−/−	6	Female	12	0.68 ± 0.02	0.77 ± 0.06

–No detectable adenine and/or 2,8-dihydroxyadenine (DHA).

[a]Urine from only one animal was analyzed here, but previous work from our laboratory has shown that wild-type male mice at 12 weeks of age have no detectable DHA in the urine, and adenine excretion is minimal ([37] and [71]).

[b]Purine excretion values were significantly higher in double knockout versus *Aprt* knockout male mice at 12 weeks of age. The respective *P* values were 0.039 for adenines/total purines and <0.001 for DHA/total adenines.

[c]There were no statistically significant differences in purine excretion between double knockout and *Aprt* knockout female mice at 12 weeks of age, even though both groups excreted adenine and DHA at levels that were comparable to those seen in 12-week-old male mice of the same genotypes.

Table 3. Pathology score in mice by age, gender, and genotype[a]

Genotype	Number	Gender	Age *weeks*	Pathology score
Aprt−/− *Opn*+/+	4	Male	6	0.3 ± 0.47
Aprt−/− *Opn*−/−	6	Male	6	0.92 ± 0.49
Aprt−/− *Opn*+/+	4	Female	6	0.88 ± 0.75
Aprt−/− *Opn*−/−	6	Female	6	0.85 ± 0.97
Aprt−/− *Opn*+/+	4	Male	12	0.9 ± 1.0
Aprt−/− *Opn*−/−	5	Male	12	2.0 ± 0.79
[b]*Aprt*−/− *Opn*+/+	5	Female	12	0.13 ± 0.25
[b]*Aprt*−/− *Opn*−/−	4	Female	12	1.72 ± 1.20

[a]All *Aprt*+/+ *Opn*+/+ and *Aprt*+/+ *Opn*−/− mice studied had pathology scores of 0 regardless of age or gender.

[b]Pathology scores in 12-week-old double knockout female mice were significantly higher than those in *Aprt* knockout female mice (*P* value 0.033).

Crystal quantification

The mean area occupied by crystal particles in six 12-week-old male mice of genotype *Aprt*−/− *Opn*−/− was compared to previously published data from our group for *Aprt*−/− *Opn*+/+ mice of the same age [43]. Considering the consistency of our prior results, in which we used mice of the same strain and age group and the same study design as in the present study, we did not find it necessary to repeat crystal quantification in *Aprt*−/− *Opn*+/+ mice [43]. The mean values were 2400 ± 1304 mm^2 and 834 ± 443 mm^2, respectively (*P* value 0.0193), indicating that double knockout mice had significantly more crystals than *Aprt* knockout mice. The corresponding values in 12-week-old female mice of genotypes *Aprt*−/− *Opn*−/− and *Aprt*−/− *Opn*+/+ were 199 ± 146 mm^2 and 159 ± 170 mm^2 (*P* value 0.37) respectively, indicating that, as with urine purine excretion, there was no significant difference in crystal burden between these two genotypes. For a given genotype, males had significantly more crystals than females, with *P* values of <0.0001 for double knockout males versus females and 0.0437 for *Aprt*−/− *Opn*+/+ males versus females. The *Opn*−/− background did not appear to affect the location of the crystals, as they were found in both groups throughout the tubules and interstitium, particularly in the cortex. As in our previous study [43], there was variation in the crystal burden in age-, gender-, and genotype-matched animals, as reflected in the observed standard deviations.

F4/80 immunohistochemistry

We scored macrophage levels in male and female mice of both age groups and all four genotypes (three to six animals per group) (Fig. 1). There was no significant difference in macrophage levels between *Aprt*+/+ *Opn*+/+ and *Aprt*+/+ *Opn*−/− mice of any age or gender, or between gender-matched groups at age 6 weeks for genotypes *Aprt*−/− *Opn*−/− and *Aprt*−/− *Opn*+/+. The difference in macrophage levels at age 12 weeks for genotype *Aprt*−/− *Opn*−/− versus *Aprt*−/− *Opn*+/+ approached statistical significance in male mice (2.3 ± 0.63 versus 1.4 ± 0.90) (*P* value 0.059) and was highly significant in female mice (2.25 ± 0.45 versus 0.92 ± 0.29) (*P* value <0.0001).

Collagen quantification

We found no significant difference in collagen levels between gender-matched groups of *Aprt*+/+ *Opn*+/+ and *Aprt*+/+ *Opn*−/− mice at any age group, or between *Aprt*−/− *Opn*−/− and *Aprt*−/− *Opn*+/+ mice at age 6 weeks. There was a statistically significant difference in collagen deposition between gender-matched groups

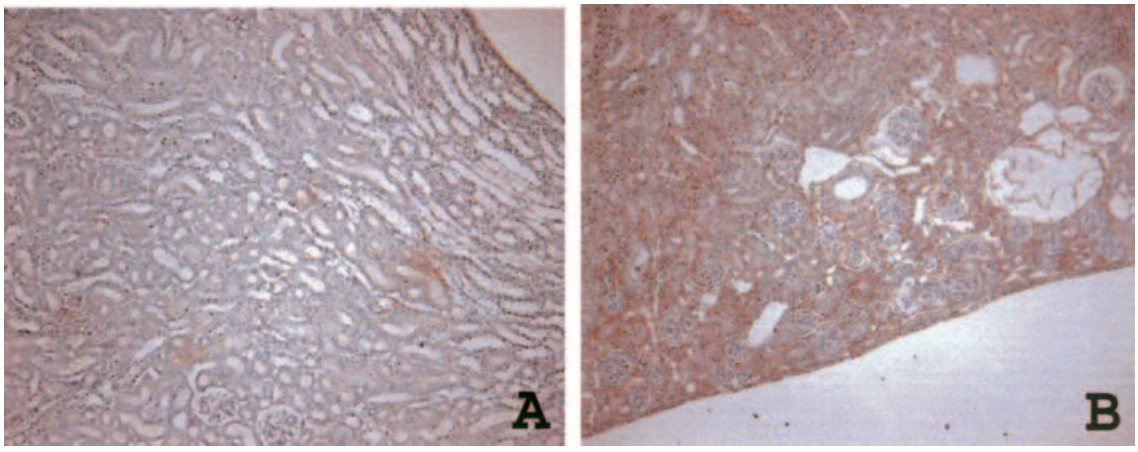

Fig. 1. Staining for macrophages using F4/80 antibody. (*A*) Twelve-week-old *Aprt*−/− *Opn*+/+ female with a macrophage score of 0.5. (*B*) Twelve-week-old *Aprt*−/− *Opn*−/− female with a macrophage score of 3.0.

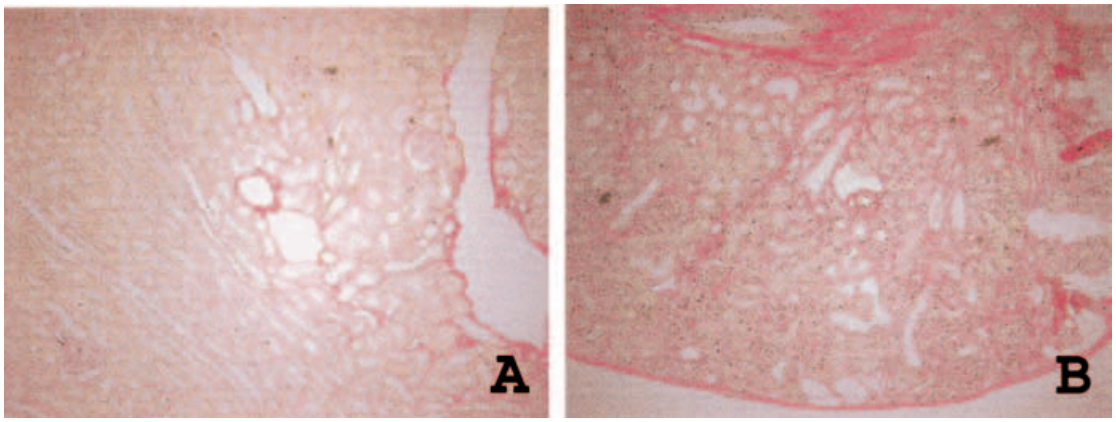

Fig. 2. Staining for collagen using picrosirius red. Collagen stains dark pink; the rest of the tissue is light pink or off-white. (*A*) A mildly affected 12-week-old *Aprt*−/− *Opn*+/+ female with a collagen content of approximately 7% of the whole section. (*B*) A severely affected 12-week-old *Aprt*−/− *Opn*−/− female with a collagen content of approximately 28% of the whole section.

of both male and female mice of genotypes *Aprt*−/− *Opn*−/− versus *Aprt*−/− *Opn*+/+ at 12 weeks of age. The values for males were 25.5 ± 11.2 versus 8.9 ± 7.9 (*P* value 0.014), and the corresponding values for females were 10.5 ± 7.4 versus 2.3 ± 1.4 (*P* value 0.025). This indicated that both male and female *Aprt*−/− *Opn*−/− mice at age 12 weeks had more severe tissue fibrosis than their *Aprt*−/− *Opn*+/+ counterparts (Fig. 2). These data also indicated that *Aprt*−/− male mice had more severe kidney fibrosis than genotype-matched females, regardless of *Opn* genotype.

XDH mRNA in situ hybridization

Macrophages contain XDH [49] and this could account, at least in part, for any observed differences in inflammation and DHA crystal deposition among genotypes. We therefore examined XDH mRNA by in situ hybridization in kidney sections from male mice of genotypes *Aprt*−/− *Opn*−/− and *Aprt*−/− *Opn*+/+ (five mice per group) at age 12 weeks and with varying degrees of macrophage infiltration. We selected these groups because they showed the greatest difference in macrophage infiltration, in urinary purine excretion, and in crystal aggregation. XDH was localized primarily in areas that were densely infiltrated by macrophages (Fig. 3) and 12-week-old *Aprt*−/− *Opn*−/− male mice showed increased XDH mRNA expression than their *Aprt*−/− *Opn*+/+ counterparts.

DISCUSSION

We observed several important differences when comparing *Aprt* knockout mice generated on an *Opn*−/− versus an *Opn*+/+ background. Over a 12-week period, *Aprt*−/− *Opn*−/− male mice had a lower maximum body weight than their *Aprt*−/− *Opn*+/+ counterparts, and female pups also had lower survival on an *Opn*−/− background. These observations combined suggest that the *Opn*−/− background in *Aprt*−/− mice have a negative effect on health and survival in both males and females. The

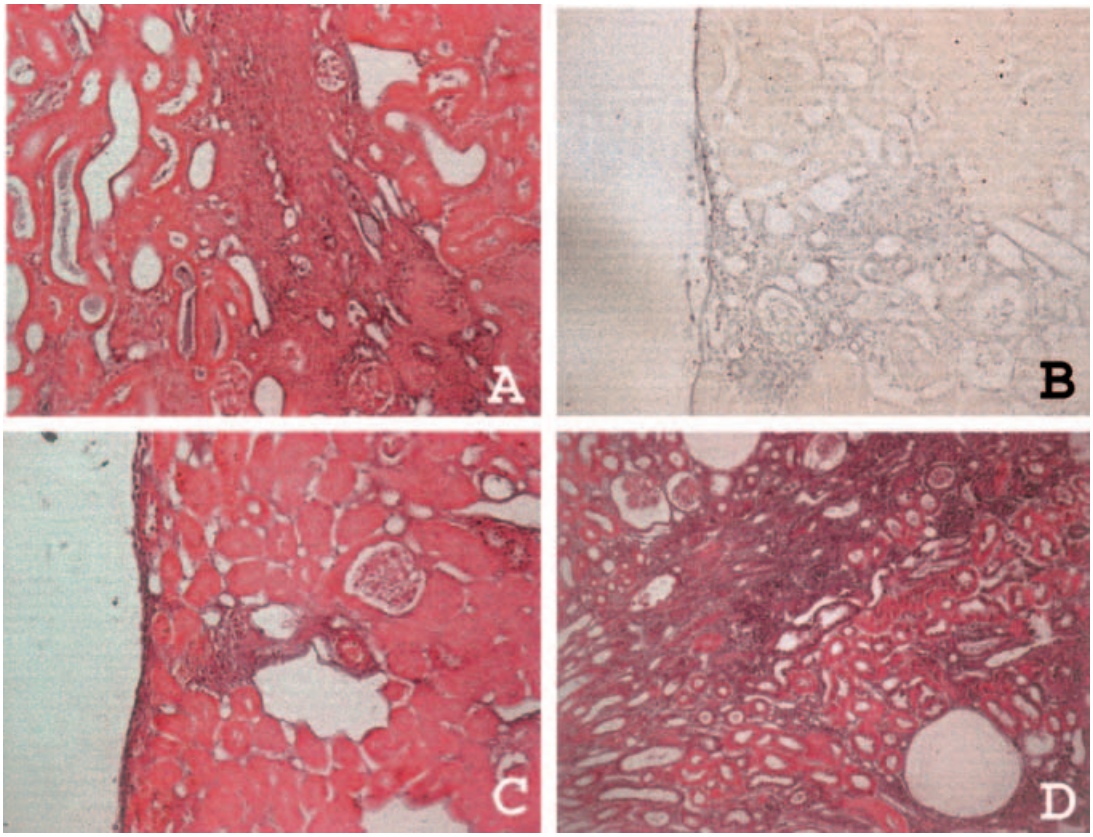

Fig. 3. Xanthine dehydrogenase expression by mRNA in situ hybridization in kidney sections from three 12-week-old double knockout male mice (*A*, *C*, and *D*) and a 12-week-old *Aprt−/−* male mouse (*B*). The signal was detected using nitro blue tetrazolium (purple). The slides were counterstained with eosin (pink), except for (B), which has no counterstain.

earliest weight data we recorded was at 4 to 6 weeks, but a recent study has shown that *Opn−/−* embryos were significantly smaller than wild-type embryos at gestational ages 10.5, 15.5, and 19.5 days [50]. The *Aprt−/− Opn−/−* embryos would be expected to be even smaller.

There was a significant difference in purine excretion, DHA crystal deposition, and renal histopathology between *Aprt−/− Opn−/−* and *Aprt−/− Opn+/+* male mice at 12 weeks. The double knockout male mice showed higher ratios of total adenines/total purines and DHA/total adenines in the urine. These higher ratios and the increased crystal burden in kidney sections are indicative of more severe stone disease in double knockout versus *Aprt−/− Opn+/+* male mice. In contrast to males, there was no significant difference in urinary purine excretion or crystal deposition between 12-week-old *Aprt−/− Opn−/−* and *Aprt−/− Opn+/+* female mice, despite the fact that both these genotypes excreted substantial amounts of adenine and DHA. This may be due to the fact that there was a relatively small amount of crystal material in kidneys from females compared with males [43]. Increased macrophage infiltration and collagen content in kidneys from *Aprt−/− Opn−/−* versus *Aprt−/− Opn+/+* female mice, despite a lack of significant difference in crystal content or purine excretion between the two groups, again suggest that OPN is a modifier of the inflammatory response. Estrogens are reported to enhance OPN expression [51], and this may account for the reduced inflammation in *Aprt−/− Opn+/+* females. Our findings also suggest that, even at comparable levels of urinary DHA, there are inherent differences in the amount of crystal deposition between male and female kidneys.

Differences in the progression of renal disease between male and female mice may reflect intrinsic differences in kidney structure and function, blood pressure, or hormonal changes, as has been suggested for humans with various forms of kidney disease [52–54]. Our previous observations of increased expression of genes related to fibrosis, tissue calcification, and transmembrane proteins in kidneys from Aprt-deficient male mice provide support for the gender bias in disease severity [41]. Also, it has been suggested in a model of renal ischemia that inducible nitric oxide synthetase (iNOS) is a crucial factor mediating the differences between male and female response to kidney injury, with testosterone inhibiting iNOS and thereby rendering the male kidney more susceptible to disease [55]. Whether this is applicable to DHA

crystal–induced injury is under investigation in our laboratory. The male kidney may be less well equipped to handle supersaturated concentrations of DHA, thus increasing DHA crystal deposition with consequent fibrosis.

At 12 weeks of age, markers of inflammation and tissue damage such as macrophage infiltration and collagen deposition were generally present at higher levels in *Aprt*−/− *Opn*−/− compared with *Aprt*−/− *Opn*+/+ mice. The fact that there was little or no difference between the genotypes at 6 weeks may at first seem puzzling, since many previous studies have shown OPN to be a promoter, rather than an inhibitor, of macrophage chemotaxis and activation but, as indicated earlier, these studies were carried out in animal models for acute renal injury [22, 28–30]. Our findings in a chronic kidney disease model over a 12-week period support a role for OPN as an inhibitor of crystal deposition, and they suggest that, at least in males, OPN may inhibit inflammation via a reduction in the stone burden. The relationship between OPN expression and crystal deposition in female mice is less well defined. We are addressing these issues using cDNA microarrays, and have to date identified a number of novel genes as well as differences in gene expression between male and female kidneys [Vernon et al, in preparation].

In addition to OPN deficiency, increased expression of XDH may also account for increased DHA crystal deposition and subsequent inflammation in *Aprt*−/− *Opn*−/− versus *Aprt*−/− *Opn*+/+ male mice. In fact, both effects may be operating in the same tissue, possibly creating a positive feedback loop with increased crystal deposition causing increased inflammation, which then causes increased infiltration by XDH-containing macrophages. In this case, the additional XDH would further convert adenine present in the tubular fluid to DHA, thus contributing to increased DHA levels in older mice and hence more kidney inflammation. However, *Aprt*−/− *Opn*−/− female mice also had increased macrophage infiltration but did not show an increase in DHA crystal deposition. Thus, the relationship between inflammation and increased XDH expression requires verification.

OPN, which is highly negatively charged [18], likely functions as an inhibitor of calcium oxalate monohydrate crystal formation via ionic interactions with the positively charged crystal substance, thereby interrupting crystal growth and accumulation. This is supported by work showing that alteration of the phosphorylation level of OPN significantly alters its ability to inhibit calcium oxalate monohydrate stone formation [56]. Other work has shown that artificially created proteins that are highly negatively charged also prevent calcium oxalate monohydrate stone formation [57]. Similar studies with DHA or other stone-forming crystals have not been carried out, but the basic nature of the 6-amino group of DHA provides one possible site for interaction with negative charges on OPN. Human urine has an enhanced capacity for solubilizing DHA [58], and supersaturation of urine with DHA has been demonstrated in some APRT-deficient patients [35]. It remains to be determined whether OPN or other macromolecules are involved in these processes. DHA stones contain trace amounts of other materials, including calcium oxalate, calcium phosphate, and UA [59, 60], and these may also modify the DHA-OPN interaction. UA lacks amino groups, and it is noteworthy that OPN had no effect on the binding of UA crystals to renal epithelial cells [61].

Inflammation is not a major characteristic of idiopathic calcium oxalate monohydrate stone disease [62]; thus, the inflammation-related effects of OPN would not be expected in this disease. However, our findings regarding OPN deficiency are applicable to metabolic disorders of stone disease such as cystinuria [63], primary hyperoxaluria [64], and UA urolithiasis [65] in which inflammation is a prominent feature. As with APRT deficiency, lack of OPN and other inhibitors of stone formation would be expected to have a negative effect on renal pathology in these diseases.

In addition to APRT deficiency, knockout mouse models have been developed for other metabolic kidney stone diseases, including calcium stones in Dent's disease [66] and type IIa Na/Pi cotransporter gene deficiency [67], cystine stones in cystinuria [68, 69], and urate stones in urate oxidase deficiency [70]. In each of these models, the stone-forming agent is different but the nature and extent of cellular injury appears to be similar in all cases. Indicators of cellular injury include crystal growth and attachment to renal tubular epithelial cells, basement membrane changes and, with advancing disease, inflammation, tissue fibrosis, and loss of renal function [43]. These observations suggest that the pathways involved in the initiation and progression of renal injury may be common to the various metabolic stone diseases. Thus, investigations in *Aprt* and *Aprt/Opn* knockout mice have implications for understanding other stone disease pathologies and for evaluating the effects of potential inhibitors of stone formation on these pathologies.

Reprint requests to Amrik Sahota, Ph.D., Department of Genetics, Nelson Laboratories, Rutgers University, 604 Allison Road, Piscataway, NJ 08854–8082.
E-mail: sahota@biology.rutgers.edu

REFERENCES

1. Grover PK, Moritz RL, Simpson RJ, Ryall RL: Inhibition of growth and aggregation of calcium oxalate crystals in vitro—A comparison of four human proteins. *Eur J Biochem* 253:637–644, 1998
2. Asplin JR, Arsenault D, Parks JH, *et al*: Contribution of human uropontin to inhibition of calcium oxalate crystallization. *Kidney Int* 53:194–199, 1998
3. Atmani F, Opalko FJ, Khan SR: Association of urinary macromolecules with calcium oxalate crystals induced in vitro in normal human and rat urine. *Urol Res* 24:45–50, 1996

4. Coe FL, Nakagawa Y, Asplin J, *et al*: Role of nephrocalcin in inhibition of calcium oxalate crystallization and nephrolithiasis. *Mineral Electrolyt Metab* 20:378–384, 1994
5. Kumar V, Farell G, Lieske JC: Whole urinary proteins coat calcium oxalate monohydrate crystals to greatly decrease their adhesion to renal cells. *J Urol* 170:1–5, 2003
6. Nakagawa Y: Properties and function of nephrocalcin: Mechanism of kidney stone inhibition or promotion. *Keio J Med* 46:1–9, 1997
7. Ryall RL, Fleming DE, Grover PK, *et al*: The hole truth: Intracrystalline proteins and calcium oxalate kidney stones. *Molec Urol* 4:391–402, 2000
8. Verkoelen CF, Schepers MS: Changing concepts in the aetiology of renal stones. *Curr Opin Urol* 10:539–544, 2000
9. Lieske JC, Leonard R, Swift H, Toback FG: Adhesion of calcium oxalate monohydrate crystals to anionic sites on the surface of renal epithelial cells. *Am J Physiol* 270:F192–F199, 1996
10. Hoyer J, Asplin J, Otvos L: Phosphorylated osteopontin peptides suppress crystallization by inhibiting the growth of calcium oxalate crystals. *Kidney Int* 60:77–83, 2001
11. Lopez CA, Hoyer JR, Wilson PD, *et al*: Heterogeneity of osteopontin expression among nephrons in mouse kidneys and enhanced expression in sclerotic glomeruli. *Lab Invest* 69:355–363, 1993
12. Hudkins KL, Giachelli CM, Cui Y, *et al*: Osteopontin expression in fetal and mature human kidney. *J Am Soc Nephrol* 10:444–457, 1999
13. Rittling SR, Denhardt DT: Osteopontin function in pathology: Lessons from osteopontin-deficient mice. *Expt Nephrol* 7:103–113, 1999
14. Kleinman JG, Bershensky A, Worcester EM, Brown D: Expression of osteopontin, a urinary inhibitor of stone mineral crystal growth, in rat kidney. *Kidney Int* 47:1585–1596, 1995
15. Yasui T, Fujita K, Sasaki S, *et al*: Expression of bone matrix proteins in urolithiasis model rats. *Urol Res* 27:255–261, 1999
16. Denhardt DT, Giachelli CM, Ritling SR: Role of osteopontin in cellular signaling and toxicant injury. *Ann Rev Pharmacol Toxicol* 41:723–749, 2001
17. Lieske JC, Leonard R, Toback FG: Adhesion of monohydrate crystals to renal epithelial cells is inhibited by specific ions. *Am J Physiol* 268:F604–F612, 1995
18. Mazzali M, Kipari T, Ophascharoensuk V, *et al*: Osteopontin—A molecule for all seasons. *Q J Med* 95:3–13, 2002
19. Umekawa T, Iguchi M, Kurita T: The effect of osteopontin immobilized collagen granules in the seed crystal method. *Urol Res* 29:282–286, 2001
20. Verhulst A, Asselman M, Pesry VP, *et al*: Crystal retention capacity of cells in the human nephron: Involvement of CD44 and its ligand hyaluronic acid and osteopontin in the transition of a crystal binding-into a nonadherent epithelium. *J Am Soc Nephrol* 13:107–115, 2003
21. Xie Y, Sakatsume M, Nishi S, *et al*: Expression, roles, receptors, and regulation of osteopontin in the kidney. *Kidney Int* 60:1645–1657, 2001
22. Weber G, Zawaideh S, Hikita S, *et al*: Phosphorylation-dependent interaction of osteopontin with its receptors regulates macrophage migration and activation. *J Leukoc Biol* 72:752–761, 2002
23. Liaw L, Birk DE, Ballas CB, *et al*: Altered wound healing in mice lacking a functional osteopontin gene (spp1). *J Clin Invest* 101:1468–1478, 1998
24. Rittling SR, Matsumoto HN, McKee MD, *et al*: Mice lacking osteopontin show normal development and bone structure but display altered osteoclast formation in vitro. *J Bone Min Res* 13:1101–1111, 1998
25. Noiri E, Dickman K, Miller F, *et al*: Reduced tolerance to acute renal ischemia in mice with a targeted disruption of the osteopontin gene. *Kidney Int* 56:74–82, 1999
26. Yoshitake H, Rittling SR, Denhardt DT, Noda M: Osteopontin-deficient mice are resistant to ovariectomy-induced bone resorption. *Proc Natl Acad Sci USA* 96:8156–8160, 1999
27. Kitahara K, Ishijama M, Rittling SR, *et al*: Osteopontin deficiency induces parathyroid hormone enhancement of cortical bone formation. *Endocrinology* 144:2132–2140, 2003
28. Persy V, Verhulst A, Ysebaert D, *et al*: Reduced postischemic macrophage infiltration and interstitial fibrosis in osteopontin knockout mice. *Kidney Int* 63:543–553, 2003
29. Ophascharoensuk V, Giachelli C, Gordon K, *et al*: Obstructive uropathy in the mouse: Role of osteopontin in interstitial fibrosis and apoptosis. *Kidney Int* 56:571–580, 1999
30. Mazzali M, Highes J, Dantas M, *et al*: Effects of cyclosporine in osteopontin null mice. *Kidney Int* 62:78–85, 2002
31. Wesson JA, Johnson RJ, Mazzali M, *et al*: Osteopontin is a critical inhibitor of calcium oxalate formation and retention in renal tubules. *J Am Soc Nephrol* 14:139–147, 2003
32. Nau GJ, Liaw L, Chupp GL, *et al*: Attenuated host resistance against *Mycobacterium bovis* BCG infection in mice lacking osteopontin. *Infect Immun* 67:4223–4230, 1999
33. Danpure CJ: Genetic disorders and urolithiasis. *Urol Clin North Am* 27:287–299, 2000
34. Langman CB: The molecular basis of kidney stones. *Curr Opin Pediatr* 16:188–193, 2004
35. Sahota AS, Tischfield JA, Kamatani N, Simmonds HA: Adenine phosphoribosyltransferase deficiency and 2,8-dihydroxyadenine lithiasis, in *The Metabolic and Molecular Bases of Inherited Disease*, 8th ed., edited by Scriver CR, Beaudet AL, Sly WS, Valle D, New York, McGraw-Hill, 2001, pp 2571–2584
36. Gelb AB, Fye KH, Tischfield JA, *et al*: Renal insufficiency secondary to 2,8-dihydroxyadenine urolithiasis. *Hum Pathol* 23:1081–1085, 1992
37. Engle SJ, Stockelman MG, Chen J, *et al*: Adenine phosphoribosyltransferase-deficient mice develop 2,8-dihydroxyadenine nephrolithiasis. *Proc Natl Acad Sci USA* 93:5307–5312, 1996
38. Stockelman MG, Lorenz JN, Smith FN, *et al*: Chronic renal failure in a mouse model of human adenine phosphoribosyltransferase deficiency. *Am J Physiol* 275:F154–F163, 1998
39. Tzortzaki EG, Glass D, Yang M, *et al*: Gender- and age-dependent changes in kidney androgen protein mRNA expression in a knockout mouse model for nephrolithiasis. *J Histochem Cytochem* 50:1663–1669, 2002
40. Tzortzaki EG, Yang M, Glass D, *et al*: Impaired expression of an organic cation transporter, *IMPT1*, in a knockout mouse model for kidney stone disease. *Urol Res* 31:257–261, 2003
41. Wang L, Raikwar N, Deng L, *et al*: Altered gene expression in kidneys of mice with 2,8-dihydroxyadenine nephrolithiasis. *Kidney Int* 58:528–536, 2000
42. Wang L, Raikwar N, Yang M, *et al*: Induction of α-catenin, integrin α_3, integrin β_6, and PDGF-B by 2,8-dihydroxyadenine crystals in cultured kidney epithelial cells. *Expt Nephrol* 10:365–373, 2002
43. Evan AP, Bledsoe SB, Connors BA, *et al*: Sequential analysis of kidney stone formation in the Aprt knockout mouse. *Kidney Int* 60:910–923, 2001
44. Curhan GC, Willett WC, Rimm EB, *et al*: Body size and risk of kidney stones. *J Am Soc Nephrol* 9:1645–1652, 1998
45. Heller HJ, Sackhaee K, Moe OW, Pak CY: Etiological role of estrogen status in renal stone formation. *J Urol* 168:1923–1927, 2002
46. Fan J, Chandhoke PS, Grampass SA: Role of sex hormones in experimental calcium oxalate nephrolithiasis. *J Am Soc Nephrol* 10 (Suppl 14):S376–S380, 1999
47. Liang L, Deng L, Shao C, *et al*: In vivo loss of heterozygosity in T-cells of B6C3F1 Aprt(+/−) mice. *Environ Mol Mutagen* 35:150–157, 2000
48. Simmonds HA, Duley JA, Davies PM: Analysis of purines and pyrimidines in blood, urine and other physiological fluids, in *Techniques in Diagnostic Human Biochemical Genetics: A Laboratory Manual*, edited by Hommes F, New York, Wiley-Liss, 1991, pp 397–424
49. Hasan NM, Cundall RB, Adams GE: Xanthine oxidase/dehydrogenase activity in intact cultured cells (in situ analysis). *Free Rad Res Comm* 16:175–182, 1992
50. Weintraub AS, Lin X, Itsovich VV, *et al*: Prenatal detection of embryo resorption in osteopontin-deficient mice using serial non-invasive magnetic resonance microscopy. *Pediatr Res* 55:419–424, 2004
51. Vanacker J-M, Pettersson K, Gustafsson J-A, Laudet V: Transcriptional targets shared by estrogen receptor-related receptors

(ERRs) and estrogen receptor (ER) α, but not by Erβ. *EMBO J* 18:4270–4279, 1999
52. Coggins CH, Lewis JB, Caggiula AW, *et al*: Differences between women and men with chronic renal disease. *Nephrol Dial Transplant* 13:1430–1437, 1998
53. Neugarten J, Acharya A, Silbiger SR: Effect of gender on the progression of nondiabetic renal disease: A meta-analysis. *J Am Soc Nephrol* 11:319–329, 2000
54. Silbiger SR, Neugarten J: The impact of gender on the progression of chronic renal failure. *Am J Kidney Dis* 25:515–533, 1995
55. Park KM, Kim JI, Ahn Y, *et al*: Testosterone is responsible for enhanced susceptibility of males to ischemic renal injury. *J Biol Chem* 279:52282–52292, 2004
56. Hoyer J, Asplin J, Otvos L: Phosphorylated osteopontin peptides suppress crystallization by inhibiting the growth of calcium oxalate crystals. *Kidney Int* 60:77–83, 2001
57. Clark R, Campbell A, Klumb L, *et al*: An electrostatic surface distribution can determine whether calcium oxalate crystal growth is promoted or inhibited. *Calc Tissue Int* 64:516–521, 1999
58. Peck C, Bailey F, Moore G: Enhanced solubility of 2,8 dihydroxyadenine (DOA) in human urine. *Transfusion* 17:383–390, 1977
59. Estepa-Maurice L, Hennequin C, Marfisi C, *et al*: Fourier transform infrared microscopy identification of crystal deposits in tissues: Clinical importance in various pathologies. *Am J Clin Path* 105:576–582, 1996
60. Szonyi P, Berenyi M, Toth J: A rare enzyme deficiency causing formation of 2,8-dihydroxyadenine (purine body) caliculi. *Int Urol Nephrol* 17:231–233, 1985
61. Koka RM, Huang E, Lieske JC: Adhesion of uric acid crystals to the surface of renal epithelial cells. *Am J Physiol* 278:F989–F998, 2000
62. Evan AP, Lingeman JE, Coe FL, *et al*: Crystal-associated nephropathy in patients with brushite nephrolithiasis. *Kidney Int* 67:576–591, 2005
63. Palacin M, Goodyer P, Nunes V, Gasparini P: Cystinuria, in *The Metabolic and Molecular Bases of Inherited Disease*, 8th ed., edited by Scriver CR, Beaudet AL, Sly WS, Valle D, New York, McGraw-Hill, 2001, pp 4909–4932
64. Danpure CJ: Primary hyperoxaluria, in *The Metabolic and Molecular Bases of Inherited Disease*, 8th ed., edited by Scriver CR, Beaudet AL, Sly WS, Valle D, New York, McGraw-Hill, 2001, pp 3323–3367
65. Becker MA: Hyperuricemia and gout, in *The Metabolic and Molecular Bases of Inherited Disease*, 8th ed., edited by Scriver CR, Beaudet AL, Sly WS, Valle D, New York, McGraw-Hill, 2001, pp 2513–2535
66. Wang SS, Devuyst O, Courtoy PJ, *et al*: Mice lacking renal chloride channel, CLC-5, are a model for Dent's disease, a nephrolithiasis disorder associated with defective receptor-mediated endocytosis. *Hum Molec Genet* 9:2937–2945, 2000
67. Chau H, El-Maadawy S, McKee MD, Tenenhouse HS: Renal calcification in mice homozygous for the disrupted type IIa Na/Pi cotransporter gene *Npt2*. *J Bone Miner Res* 18:644–657, 2003
68. Feliubadalo L, Arbones ML, Manas L, *et al*: Slc7a9-deficient mice develop cystinuria non-I and cystine urolithiasis. *Hum Molec Genet* 12:2097–2108, 2003
69. Peters T, Thaete C, Wolf S, *et al*: A mouse model for cystinuria type 1. *Hum Molec Genet* 12:2109–2120, 2003
70. Wu X, Wakamiya M, Vaishnav S, *et al*: Hyperuricemia and urate nephropathy in urate oxidase-deficient mice. *Proc Natl Acad Sci USA* 91:742–746, 1994
71. Engle SJ, Womer DE, Davies PM, *et al*: HPRT-APRT-deficient mice are not a model for Lesch-Nyhan syndrome. *Hum Mol Genet* 5:1607–1610, 1996